Mass Transfer at High Péclet Numbers for Creeping Flow in a Packed-Bed Reactor

PETER FEDKIW
and
JOHN NEWMAN

Materials and Molecular Research Division
Lawrence Berkeley Laboratory and
Department of Chemical Engineering
University of California
Berkeley, California 94720

An isotropic, homogeneous packed-bed reactor is modeled as an array of sinusoidal periodically constricted tubes (PCT). The effective asymptotic bed-Sherwood number has been calculated for mass transfer at large Péclet number with a constant wall concentration and creeping flow hydrodynamics. The bed friction factor has also been calculated. The results for these macroscopic bed quantities depend upon two ratios of the microscopic PCT period length, average radius, and sinusoidal amptitude.

SCOPE

The mass transfer rate occurring across a packed-bed reactor can be predicted a priori if the exact geometry of the flow channels is known. This is usually impossible except for a uniformly structured bed. It then becomes necessary to introduce microscopic channel models for the bed. The simplest model considers the bed to be an array of straight cylinders. A higher-order approximation accounts for the fact that the straight conduit model cannot reproduce the contortions the fluid must pass through in the bed. A periodically constricted tube (PCT) model of a bed, however, is a step in this realization. The converging, diverging character of the flow in these tubes is a better approximation to the true nature of the flow in the actual bed.

Using the PCT model for the flow channels in a bed, the appropriate governing equations can then be solved for the effective bed-Sherwood number. Specifically, the Navier-Stokes equations must first be solved for the velocity field which is then used in the convective diffusion equation to solve for the reactant concentration profile. This paper presents results for the friction factor and the Sherwood number of a deep bed modeled as an array of sinusoidal PCT. Creeping flow has been assumed, and the wall concentration of the reactant is constant through the depth of the bed. Since the Schmidt number for liquid reactants is high, a large reactant Peclet number is assumed in the analysis.

CONCLUSIONS AND SIGNIFICANCE

A homogeneous, isotropic packed-bed reactor can be modeled as an array of periodically constricted tubes. By neglect of entrance region effects, the governing equations for fluid flow and mass transport need only be solved in a single period owing to the assumed homogeneity of the bed.

Interior collocation on a finite-difference grid was used to reduce the creeping flow, Stokes, stream function equation in a sinusoidal PCT to a set of coupled, fourth-order, ordinary differential equations. This approach is much more economical than solving the full eliptic partial differential equation by overrelaxation.

At a high reactant Péclet number in the fully developed mass transfer region, the convective diffusion equation for the reactant in a PCT can be reduced to a Graetzlike eigenvalue problem. This technique is valid for laminar flow in any PCT.

Figure 9 shows the friction factor, Reynolds number product in creeping flow for a packed bed modeled as an array of sinusoidal PCT. The results depend upon the two dimensionless geometric variables r_A and A/r_A (Figure 2). As the average wall radius decreases, or as the amptitude increases, the product increases.

Results are presented in Figure 11 for the asymptotic Sherwood number of a deep-bed reactor with a large reactant Péclet number in creeping flow. Again, the results depend upon the two dimensionless geometric variables. The bed-Sherwood number exhibits different behavior in the amplitude-radius ratio (A/r_A) for small and large values of r_A. In beds of long skinny tubes (small r_A), the Sherwood number increases with A/r_A, whereas for larger r_A this trend reverses itself.

The flow channels in a randomly packed bed defy an analytic expression. To predict a priori the transfer rates in a bed, it becomes necessary to resort to empirical correlations or, alternatively, to a microscopic model for the flow channels. The appropriate rate equations can be solved within the framework of the model to predict the performance of a bed. Of course, the structured formulation of a microscopic channel model is a framework to understand better the empirical correlations.

The simplest model of a bed considers the flow channels to be an array of straight tube capillaries embedded in an impermeable matrix. Sheidegger (1957) and more recently Dullien (1975) have provided a review of this approach. Such a first-order approach cannot, how-

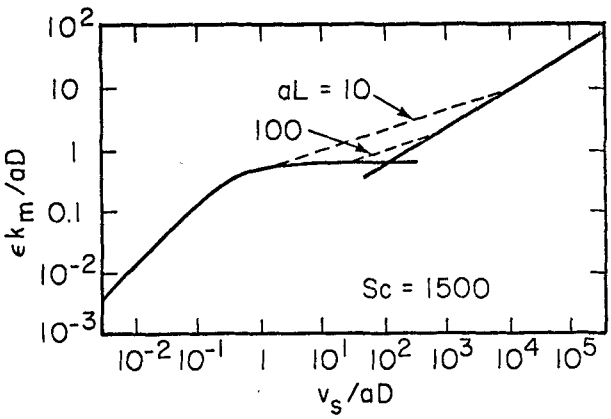

Fig. 1. Expected behavior of bed-Sherwood number.

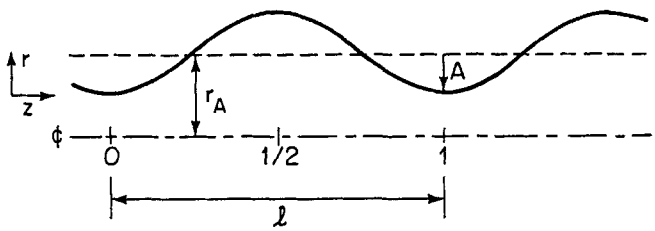

Fig. 2. The wall of a PCT generated by $r_w(z) = r_A - A \cos(2\pi z)$. All lengths are dimensionless with respect to the period length l.

ever, without the introduction of another parameter, satisfactorily correlate experimental data. The straight streamlines which result from applying the capillary model seem to be an inappropriate approximation to the twisting, converging, diverging character of the flow in an actual bed. This undulating character of the flow can have tremendous consequences on the bed pressure drop and the fluid-to-particle (or vice versa) mass transfer rates.

Petersen's (1958) work suggested that the flow channels in a bed can be modeled as an array of periodically constricted tubes (PCT). Michaels (1959), Houpeurt (1959), Batra et al. (1970), Dullien and Azzam (1973), Payatakes et al. (1973), and Sheffield and Metzner (1976) have contributed to this line of thought. The converging, diverging nature of the flow in these model tubes is a better approximation to the true character of the flow in the bed. Payatakes et al. have argued by statistical and heuristic means that the problem of modeling the flow behavior in an array of randomly sized PCT reduces to considering a single dimensionless PCT. They've presented a technique to calculate the PCT model parameters.

Having a flow channel model in hand, one can then proceed to calculate the pressure drop and the reactant concentration profile across a packed-bed reactor. Specifically, the Navier-Stokes equation must be solved first for the velocity field (neglecting free convection); and then the convective-diffusion equation must be solved for the concentration profile of each reactant. Payatakes et al. have outlined a technique for solving the full Navier-Stokes equations in a PCT. No work to the authors' knowledge has been done on the mass transfer problem in a packed-bed reactor modeled as an array of these PCT. In this work, we have calculated the asymptotic, creeping flow Sherwood number (based on a logarithmic mean concentration driving force) for a single limiting reactant with a high Péclet number. Physically, these restrictions correspond to a liquid reactant flowing through a deep bed at a low Reynolds number. The reactant wall concentration is assumed constant throughout the length of the reactor, corresponding to a limiting current condition.

The behavior of the effective mass transfer coefficient through a packed bed depends upon the flow regime. For a deep bed, the effective mass transfer coefficient in creeping flow will become independent of the velocity. This is in contrast to the entry region where the transfer rate is proportional to the velocity to the one third power. The entry region has an effective transfer coefficient larger than that for deeper beds. Calculation of the deep-bed asymptotic Sherwood number thus gives a lower limit to the expected behavior. The horizontal line of Figure 1 shows the nature of this Sherwood number. The dashed lines indicate entry region coefficients for two different sized beds. The line marked $aL = 10$ is the Wilson-Geankopolis (1966) correlation. The left- and right-hand sides of this figure indicate schematically regions where axial diffusion and turbulent convection, respectively, become important. The turbulent region line is a plot of the Bird et al. (1960) correlation, while the low Péclet number region is a plot of Sørenson and Stewart's (1974*b*) calculations for a simple cubic packed bed of spheres.

MATHEMATICAL MODELING

Creeping Flow in a PCT

The PCT considered is generated by the surface of revolution of a cosine function about the axis of symmetry as shown in Figure 2. All lengths are made dimensionless with the period of oscillation l. The creeping flow equations are to be solved in this geometry. Because no inertial effects are present and the tube wall is axially symmetric at $z = 0$, 0.5, and 1, the radial velocity v_r will be zero at these same positions. It then follows that the streamwise velocity v_ξ will be an even periodic function of z with the same frequency as the wall oscillation. These considerations make it clear that the governing equations need be only solved in $0 \leq z \leq 0.5$ for this particular geometry.

A packed bed is modeled as an array of these PCT. The fluid approaches the bed at a superficial approach velocity v_s. The average dimensional velocity $\langle v_{Ad} \rangle$ through each tube is defined such that the flow rate in each tube is equal to $\langle v_{Ad} \rangle \pi r^2_{Ad}$, where r_{Ad} is the length averaged dimensional radius. Geometrical considerations show that $\langle v_{Ad} \rangle$ can be written in terms of the approach velocity as

$$\langle v_{Ad} \rangle = \frac{v_s}{\epsilon}\left[1 + \frac{1}{2}(A/r_A)^2\right]$$

where A is the dimensionless wall oscillation amplitude. The governing equations need be solved in a single PCT. These results can then be applied to the entire bed owing to the assumed homogeneity and periodicity of the structure.

The dimensionless, incompressible Navier-Stokes equations for creeping flow with axial symmetry can be reduced to a single, linear, fourth-order partial differential equation by introducing the normalized stream function ψ as

$$E^4\psi = 0 \tag{1}$$

where

$$E^2 = \frac{\partial^2}{\partial r^2} - \frac{1}{r}\frac{\partial}{\partial r} + \frac{\partial^2}{\partial z^2} \tag{2}$$

$$v_z = \frac{r_A^2}{2r}\frac{\partial \psi}{\partial r} \tag{3}$$

$$v_r = -\frac{r_A^2}{2r}\frac{\partial\psi}{\partial z}$$

The stream function equation is to be solved subject to the boundary conditions

$$\left.\begin{aligned}\psi &= 0 \qquad (4a)\\ \frac{\partial}{\partial r}\frac{1}{r}\frac{\partial\psi}{\partial r} &= 0 \qquad (4b)\end{aligned}\right\} r = 0$$

$$\left.\begin{aligned}\frac{1}{r}\frac{\partial\psi}{\partial r} &= 0 \qquad (4c)\\ \psi &= 1 \qquad (4d)\end{aligned}\right\} r = r_w(z)$$

and a periodicity condition

$$\frac{\partial^{(n)}}{\partial z^{(n)}}\psi(r,z) = \frac{\partial^{(n)}}{\partial z^{(n)}}\psi(r, z+m)n, m = 0, 1, 2, \ldots \qquad (5)$$

The boundary conditions of Equation (4) state that at the center line the radial velocity is zero and the axial velocity is symmetric, and at the wall there is no slip on the axial velocity and the flow rate at each cross section is a constant, here referred to a straight cylinder of radius r_A.

No analytic solution for Equations (1), (4), and (5) could be found. Interior collocation on a finite-difference grid was used to generate an approximate solution. The collocation approximation technique is examined by Finlayson (1972), Villadsen (1970), and Villadsen and Stewart (1967).

A transformed radial coordinate η is introduced by

$$\eta = r/r_w(z) \qquad (6)$$

The boundary conditions of Equation (4) along the wall are then transferred to the coordinate curve $\eta = 1$. In this new coordinate, the interior collocation technique on a finite-difference grid can be used to approximate the hydrodynamics. Assume a solution for the normalized stream function of the form

$$\psi(\eta, z) = 2\eta^2 - \eta^4 + \sum_{k=1}^{NCP} \eta^2(1-\eta^2)^2 A_k(z)\phi_{k-1}(\eta^2) \qquad (7)$$

The first two terms on the right side represent the Hagen-Poiseuille solution. The summation of terms can then be considered as a correction function to the basic parabolic flow. The functions $\phi_{k-1}(\eta^2)$ in the summation term can be any complete set of functions. The weighting factor $\eta^2(1-\eta^2)^2$ assures the correct behavior of the solution at the boundary points $\eta = 0$ and $\eta = 1$. The coefficients $A_k(z)$ are unknown functions of z to be determined subject to the boundary conditions

$$\begin{aligned}A_k'(0) &= A_k'''(0) = 0\\ A_k'(0.5) &= A_k'''(0.5) = 0\end{aligned} \qquad (8)$$

These conditions result from the periodic, symmetric tube wall. In noncreeping flow, these coefficients would not identically equal zero but some constant which must be determined as part of the solution.

A friction factor for a packed bed may be defined as

$$f_B = \frac{36\epsilon^3}{a}\left(\frac{-\Delta\mathcal{P}_B}{L_B}\right)\frac{1}{\rho v_s^2} \qquad (9)$$

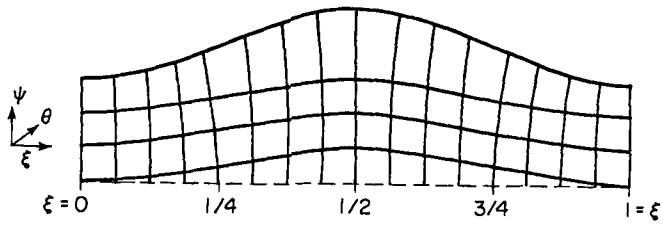

Fig. 3. The (ψ, ξ, θ) coordinate system.

A porosity dependence has been explicitly incorporated into this definition. For creeping flow, the product of the Reynolds number and the bed friction factor is a constant given by

$$f_B Re_B = 72\left(\frac{2\epsilon}{ar_{Ad}}\right)^2\left[1 + \frac{1}{2}(A/r_A)^2\right]\int_0^1 \left(\frac{r_A}{r_w}\right)^4 \left\{1 + \sum_{k=1}^{NCP} A_k(z)[2\phi_{k-1}(0) - \phi''_{k-1}(0)/2]\right\} dz \qquad (10)$$

This equation was derived by integrating the pressure gradient in the Navier-Stokes equations over a period at the center line. The left side of Equation (10) depends upon the macroscopic bed quantities, while the right side depends upon the microscopic model parameters r_A and A/r_A only.

Convective Diffusion Equation at High Peclet Numbers

The dimensionless, steady state, convective-diffusion equation for a single limiting reactant can be written in generalized vector notation as

$$\bar{v}\cdot\nabla C = \frac{2r_A}{Pe}\nabla^2 C \qquad (11)$$

This equation with a creeping flow velocity profile is to be solved in the far downstream region of a PCT for the asymptotic solution as $Pe \to \infty$. Solving this equation in a straight tube after neglecting diffusion in the axial direction, we obtain the well-known Graetz solution. At high Pe it is also valid to neglect diffusion parallel to the streamwise velocity in a PCT.

It is convenient to solve Equation (11) in a transformed coordinate system (ψ, ξ, θ) (Figure 3). The ψ coordinate is constant along streamlines and is found directly from the stream function. The ξ direction is parallel to the streamwise velocity at all positions and is scaled such that $\xi = 0$ at the beginning of a period and $\xi = 1$ at the end. It is defined implicitly by $(\nabla\psi)\cdot(\nabla\xi) = 0$. The angular coordinate θ has its usual meaning. In this coordinate system, diffusion will be important in the ψ direction and negligible in the ξ direction, at high Péclet numbers.

With neglect of diffusion in the ξ direction, Equation (11) can be written as

$$\frac{v_\xi}{h_\xi}\frac{\partial C}{\partial\xi} = \frac{2r_A}{Pe}\frac{1}{h_\theta h_\psi h_\xi}\frac{\partial}{\partial\psi}\left(\frac{h_\theta h_\xi}{h_\psi}\frac{\partial C}{\partial\psi}\right) \qquad (12)$$

Explicit forms for two of the metric factors can be determined. By inspection, $h_\theta = r$. Since the stream function represents the amount of fluid flowing in a stream tube between a point and the axis

$$\psi = \frac{2}{r_A^2}\int_0^\psi v_\xi r h_\psi d\psi \qquad (13)$$

after appropriate normalization. It follows that the metric

factor h_ψ is related to the streamwise velocity v_ξ:

$$h_\psi = \frac{r_A^2}{2r}\frac{1}{v_\xi} \tag{14}$$

Equation (12) now becomes

$$\frac{\partial C}{\partial \xi} = \frac{8}{r_A Pe}\frac{\partial}{\partial \psi}\left[(r/r_A)^2 v_\xi h_\xi \frac{\partial C}{\partial \psi}\right] \tag{15}$$

which applies to any PCT.

Unfortunately, Equation (15) cannot be solved by a separation of variables technique. One can, however, formulate a perturbation solution to Equation (15) in the deep region of the bed where the entrance effects have been damped. Equation (15) suggests as a first approximation

$$\frac{\partial C}{\partial \xi} = 0 \tag{16}$$

at large Pe. This would imply that the concentration is a function of ψ only and is constant along a streamline. Any function of ψ will suffice. The first-order term in the perturbation solution should then be a function of ψ. The second-order term will then be a diffusive correction function to take into account that the concentration must also be changing in the ξ coordinate. Assume a solution of the form

$$C(\psi, \xi) = C_1(\psi) + C_2(\psi, \xi) \tag{17}$$

Substitution of Equation (17) into Equation (15) yields

$$\frac{\partial C_2}{\partial \xi} = \frac{8}{r_A Pe}\frac{\partial}{\partial \psi}\left[(r/r_A)^2 v_\xi h_\xi \frac{\partial C_1}{\partial \psi}\right] \tag{18}$$

after neglect of the diffusive term in C_2.

In the far downstream region of a PCT, the fractional decrease of concentration through each period must be the same; that is

$$C(\psi, \xi + 1) = C(\psi, \xi)e^{-\beta l} \tag{19}$$

where β is independent of position. If we set $C_2(\psi, 0) = 0$, this means that C_2 and C_1 are related:

$$C_2(\psi, 1) = C_1(\psi)(e^{-\beta l} - 1) \tag{20}$$

Equation (18) can now be integrated from $\xi = 0$ to $\xi = 1$ to obtain a Sturm-Liouville eigenvalue problem for the function $C_1(\psi)$:

$$\frac{d}{d\psi}\left(G(\psi)\frac{dC_1}{d\psi}\right) + \lambda C_1 = 0 \tag{21}$$

$$G(\psi) = \int_0^1 (r/r_A)^2 v_\xi h_\xi d\xi \tag{22}$$

$$\lambda = (1 - e^{-\beta l})\frac{r_A Pe}{8} \cong \beta l \frac{r_A Pe}{8} \tag{23}$$

The integral in Equation (22) is carried out over the arc length for a constant value of ψ in the integrand. The second identification of λ to βl in Equation (23) is possible, since $Pe \to \infty$.

Equation (21) is to be solved subject to the conditions

$$C_1(0) = 1 \tag{24a}$$

$$C_1(1) = 0 \tag{24b}$$

$$C_1'(0) = -\lambda/G'(0) \tag{24c}$$

Equation (24a) is a normalization for the first-order solution. Equation (24b) satisfies the limiting reactant constraint of a zero wall concentration. Equation (24c) results from the fact that the concentration must be finite on the center line, a singular point of Equation (21).

The first eigenvalue of Equation (21) can be related to the effective Sherwood number for a deep porous bed which is modeled as an array of PCT. A macroscopic mass balance on the reactant over the length of the period can be written in terms of an effective mass transfer coefficient k_m (Newman and Tiedemann, 1976; Bennion and Newman, 1972). The β in Equation (20) can then be related to this coefficient as

$$\beta = k_m a/v_s \tag{25}$$

With Equations (25) and (23), the Sherwood number for a limiting reactant in a deep bed with creeping flow and high Péclet number can be written as

$$Sh_B = \frac{\epsilon}{a}\frac{k_m}{D} = \lambda\left[\frac{2\epsilon}{a r_{Ad}\sqrt{1 + (1/2)(A/r_A)^2}}\right]^2 \tag{26}$$

Equations (26) and (21) are the main results of this analysis. By means of the perturbation approach, we have demonstrated how the two-dimensional, convective-diffusion equation in a PCT can be reduced to a Graetz-like eigenvalue problem at high Péclet numbers. The first eigenvalue of this problem is simply related to the bed-Sherwood number as given in Equation (26).

The eigenfunction $C_1(\psi)$ generated by the perturbation analysis is a first-order approximation to the concentration distribution. It identically satisfies Equation (16) and gives the correct integral properties to the correction function $C_2(\psi, \xi)$. The local transfer rate to the wall can be found by differentiation of this profile with respect to the normal distance from the wall. After a change in coordinate system, the analysis yields

$$\left.\frac{\partial C}{\partial n}\right|_w = -\frac{\sqrt{B(z) r_w(z)}}{2r_A}\left.\frac{dC_1}{d\rho}\right|_{\rho=1} \tag{27}$$

where

$$B(z) = \left.\frac{\partial v_\xi}{\partial n}\right|_w$$

The local wall flux is thus proportional to the square root of the local shear rate. The integral of Equation (27) over the surface area of a period is related to the eigenvalue.

The left side of Equation (26) depends upon the macroscopic bed quantities a and ϵ. The right side is a function of PCT geometry and flow regime through the dependence on λ. The eigenvalues of Equation (21) are independent of the Péclet number in creeping flow. Thus, irrespective of curvature effects, the asymptotic Sherwood number is a constant independent of the Péclet number for a deep bed.

METHOD OF SOLUTION

The unknown coefficients $A_k(z)$ in the interior-collocation approximation for the stream function can be determined as follows. Equation (1) in the (η, z) coordinate system is applied to Equation (7). [The E^4 operator in the (η, z) coordinate system is given in the appendix.] Interior collocation is then used at NCP points in the η coordinate. Since the η function dependence is a priori postulated through the $\phi_{k-1}(\eta^2)$, this step reduces the partial differential equation to a set of coupled, fourth-order, ordinary differential equations for the unknown A_k. This set of equations is solved on a finite-difference grid in the z coordinate by the method of

Newman (1973*a*). Legendre polynomials were used for the $\phi_{k-1}(\eta^2)$. The η collocation points were chosen to be the zeros of the shifted Legendre polynomials of order NCP-1:

$$\eta_i = \sqrt{\frac{x_i + 1}{2}}$$

where x_i is the zero of the ordinary Legendre polynomial. The wall $\eta = 1$ was also used as a collocation point.

The eigenvalue problem as posed in Equations (21) thru (24) is ill suited numerically to the ψ coordinate. Equation (21) has two singular points, one at $\psi = 0$ and the other at $\psi = 1$. The singularity at $\psi = 0$ presents no problems; however, that at $\psi = 1$ does. An analysis of Equation (21) near the point $\psi = 1$ indicates that the first derivative of C_1 approaches infinity. A change in coordinate will eliminate this singularity. Define a lengthlike transformation variable ρ as

$$\psi = 2\rho^2 - \rho^4 \tag{28}$$

Equation (21) and its boundary conditions then transform as

$$\frac{d}{d\rho}\left(\frac{G(\psi(\rho))}{4\rho(1-\rho^2)}\frac{dC_1}{d\rho}\right) + 4\lambda\rho(1-\rho^2)C_1 = 0 \tag{29}$$

$$C_1(\rho = 0) = 1 \tag{30a}$$

$$C_1(\rho = 1) = 0 \tag{30b}$$

$$\frac{d}{d\rho}C_1(\rho = 0) = 0 \tag{30c}$$

Equations (29) and (30) were solved by the method suggested by Newman (1973*b*) for eigenvalue problems.

All calculations were done on a CDC 7600 computer. Further details of the analysis and numerical programs have been compiled by Fedkiw.

RESULTS AND DISCUSSION

The hydrodynamic results will be discussed first, followed by the mass transfer problem.

The interior-collocation solution technique for stream function required a maximum of nine (NCP = 9) η collocation points to insure sufficient accuracy of the solution. It was found that more collocation points were required as the dimensionless wall radius was increased, nine being the maximum for the most extreme case considered ($r_A = 0.5$, $A/r_A = 0.5$). Since this approximation solution is solved in a generalized (η, z) coordinate system, it facilitates a straightforward calculation for the velocity field in any tube in the shape of a periodic body of revolution. The reduction of the eliptic partial differential equation to a set of coupled ordinary equations is more economical to solve in terms of computer time usage.

A boundary-collocation solution technique was also attempted but was discarded. The general solutions (by separation of variables) to Equation (1) involve modified Bessel functions of the first kind. Unfortunately, these functions do not form a complete set, and the correction function expansion technique similar to Equation (7) did not converge.

Figure 4 shows a comparison between the creeping flow axial velocity profile calculated here and that reported by Payatakes et al. for a tube Reynolds number equal to 1. The profiles are compared at the minimum and maximum ($z = 0.5$) constriction diameters. The tube wall for these profiles is generated by two parabolas

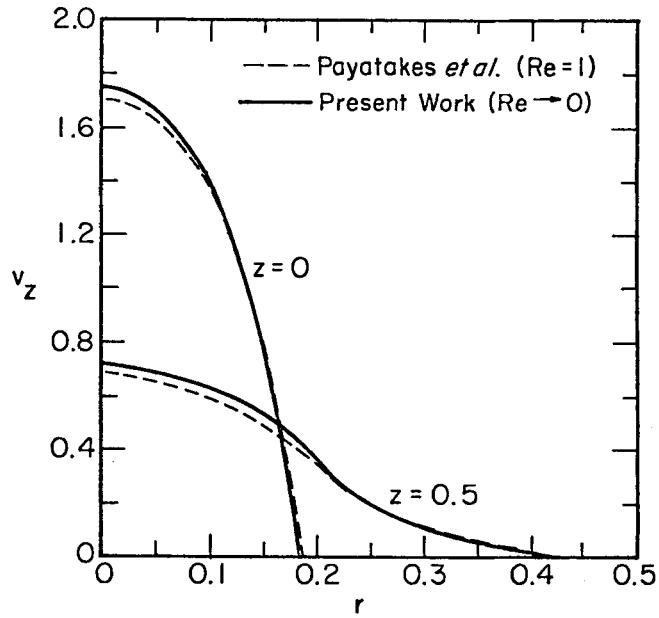

Fig. 4. Comparison of calculated axial velocity profiles with those of Payatakes et al. for a parabolic PCT.

intersecting at $z = 0.5$ with their respective minima at $z = 0$ and $z = 1$ (see Figure 1 of Payatakes et al.). The boundary conditions for the A_k's in Equation (8) were at $z = 0$ and 1.0 for this situation. The velocity here is

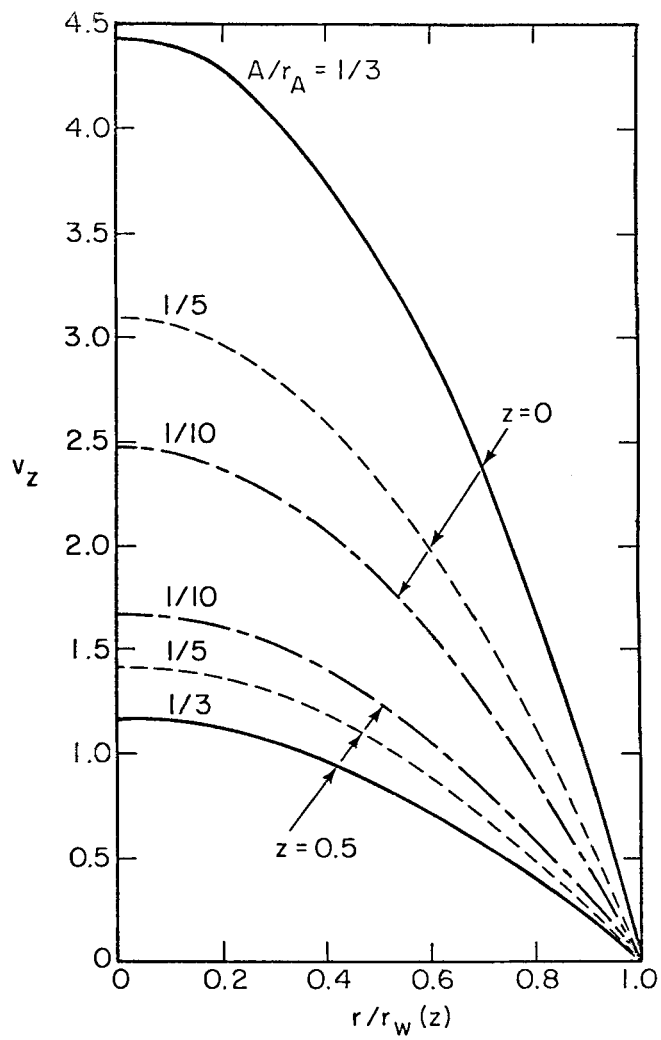

Fig. 5. Effect of amplitude/radius ratio on axial velocity profiles for a sinusoidal PCT with $r_A = 0.1$.

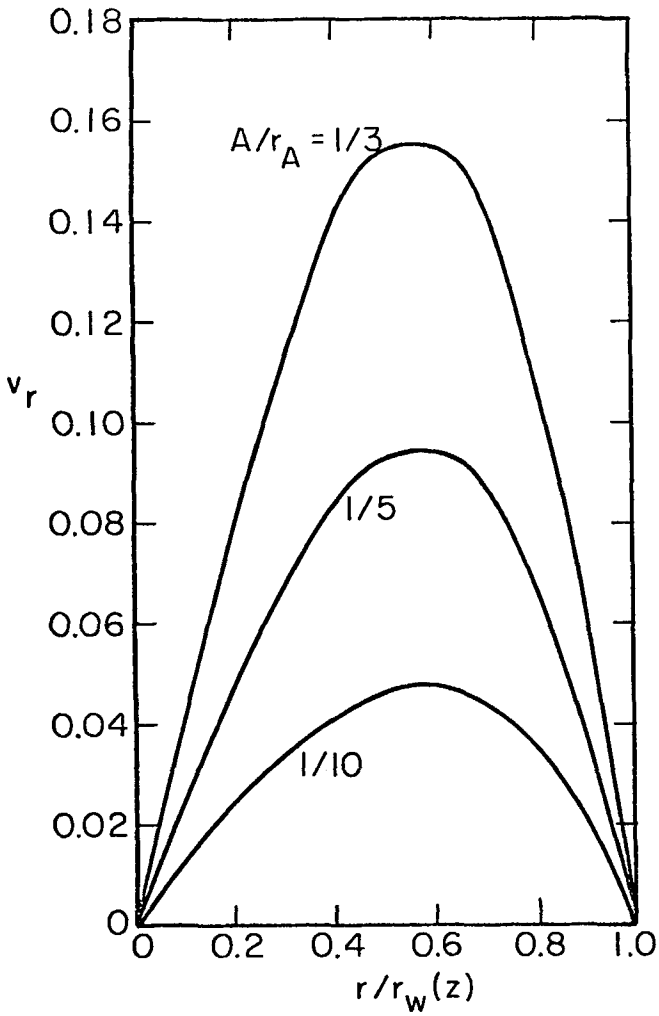

Fig. 6. Effect of amplitude/radius ratio on radial velocity profiles in a sinusoidal PCT for $r_A = 0.1$ at $z = 0.25$.

scaled with respect to the average velocity in a tube of constant radius equal to the constriction radius. At the center line, the viscous flow profile is slightly larger than that of Payatakes et al. calculations. However, near the wall this trend is reversed. The integral of all the profiles is equal to a constant defined by the flow rate.

Figures 5 thru 8 show some typical creeping flow profiles in a sinusoidal PCT. The two dimensionless geometry groups r_A and A/r_A completely determine the solution behavior. These four figures illustrate the effect on the velocity profiles of manipulating one of these variables with the other held constant. The velocity profiles have been normalized with the average velocity at the average radius.

The effect on the axial and radial velocity profiles of varying the wall amplitude at a constant average radius is shown in Figures 5 and 6. The radial velocity profile is plotted at $z = 0.25$. At this position, v_r attains its maximum value. These figures indicate that at a constant radius the variation in the velocity profiles across a half period becomes more dramatic as the oscillation amplitude increases.

Figure 7 and 8 illustrate the velocity profiles for a varying wall radius at a constant A/r_A. The effect of the tube geometry is again seen. The radial velocity increases with r_A, since the velocity of the fluid in the radial direction is proportional to the slope of the wall. However, the variations in the axial velocity profiles across the half period become less pronounced with increasing r_A. This effect is due to the drag induced by the wall. As r_A increases, the effect of the wall fluctuations become less important to the fluid in the central core of the tube.

The profiles of Figures 5 thru 8 have been nondimensionalized with respect to the average axial velocity at the average tube radius. This normalization procedure illustrates the variation of the profiles from that at the average tube radius. If these profiles are multiplied by $[r_w(z)/r_A]^2$, the resulting profiles are then normalized by the average axial velocity at position z. Such a calculation shows that the parabolic axial velocity profile is approached as r_A becomes smaller. The radial velocity profile is then given by continuity. In the limit of $r_A \to 0$, the Hagen-Poiseuille case is recovered.

Figure 9 illustrates the bed friction factor-Reynolds number product of Equation (10) as a function of r_A and A/r_A. The product $f_B Re_B$ involves the macroscopic bed parameters L_B, ϵ, and a. The microscopic PCT parameters r_A and A/r_A can be varied while these bed parameters are held constant. As A/r_A increases, the tubes become more narrow at their constrictions. Because of the increased resistance this reduced flow area offers, the bed pressure drop increases with A/r_A. This effect decreases with larger r_A, since the constriction size at any A/r_A increases with r_A.

The relative insensitivity of $f_B Re_B$ with r_A seen in Figure 9 supports the approximation of assuming that the Hagen-Poiseuille pressure gradient-flow rate relationship holds locally for sinusoidal PCT. This approximation was used by Sheffield and Metzner (1976).

The Blake-Kozeny equation as given in Bird et al. (1960) empirically recommends a value of 150 for the product $f_B Re_B$. Sørenson and Stewart (1974) have calculated the velocity profiles across a simple cubic packing of uniformly sized spheres. Their pressure drop results yield a theoretical value of 158. Figure 9 shows that a range of parameters (r_A, A/r_A) will give a $f_B Re_B$ near these two values. The A/r_A ratio which gives $f_B Re_B$ a value near 150 seem to be concentrated near 0.33.

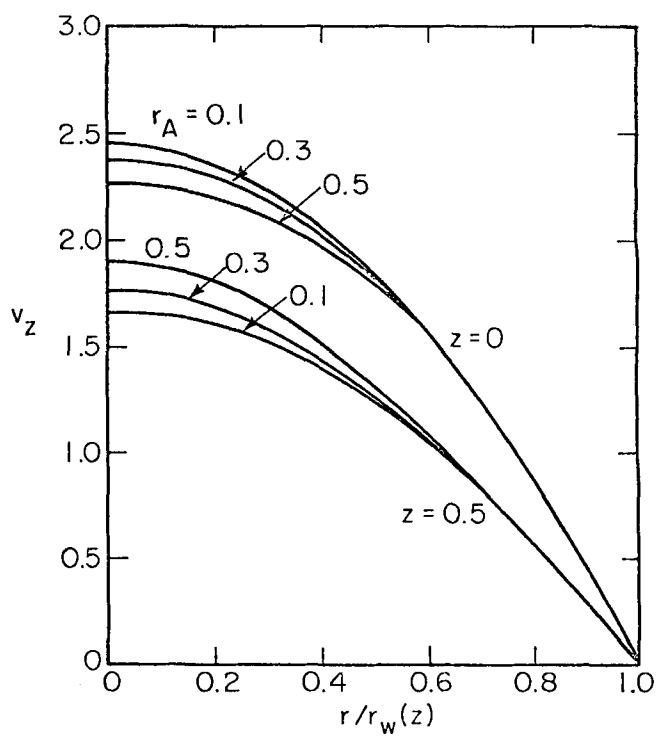

Fig. 7. Effect of average tube radius on axial velocity profiles in a sinusoidal PCT for $A/r_A = 0.1$.

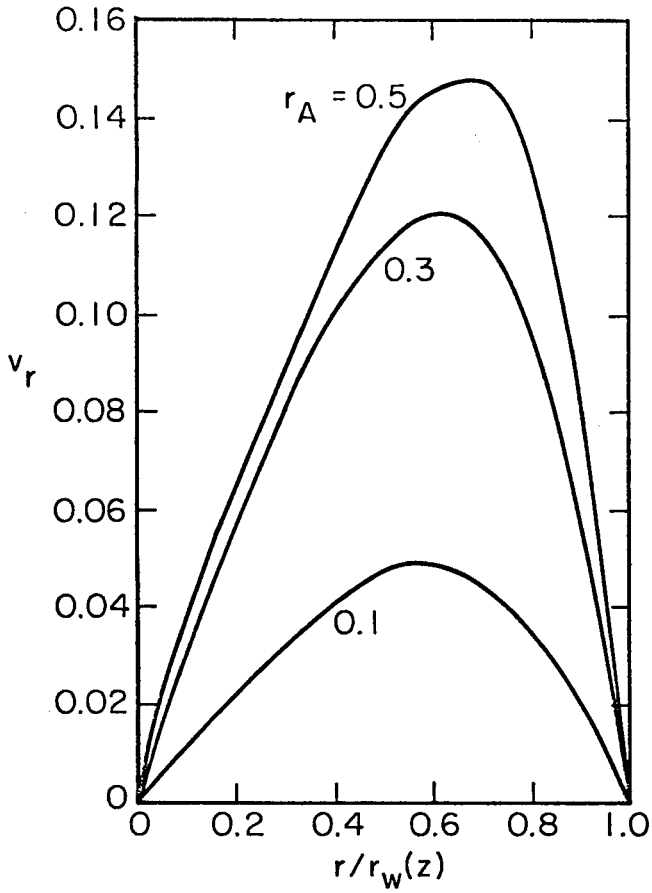

Fig. 8. Effect of average tube radius on radial velocity profiles in a sinusoidal PCT for $A/r_A = 0.1$ at $z = 0.25$.

The straight tube capillary model gives the intercept value of 72 on Figure 9. The usual argument given in explaining the discrepancy between this value and the empirically best fit value of 150 is a tortuosity and shape factor. The PCT model of a packed bed does not resort to these factors. However, another geometrical parameter (A/r_A) has been added.

The mass transfer analysis presented in this work can be used to calculate the high Péclet number asymptotic

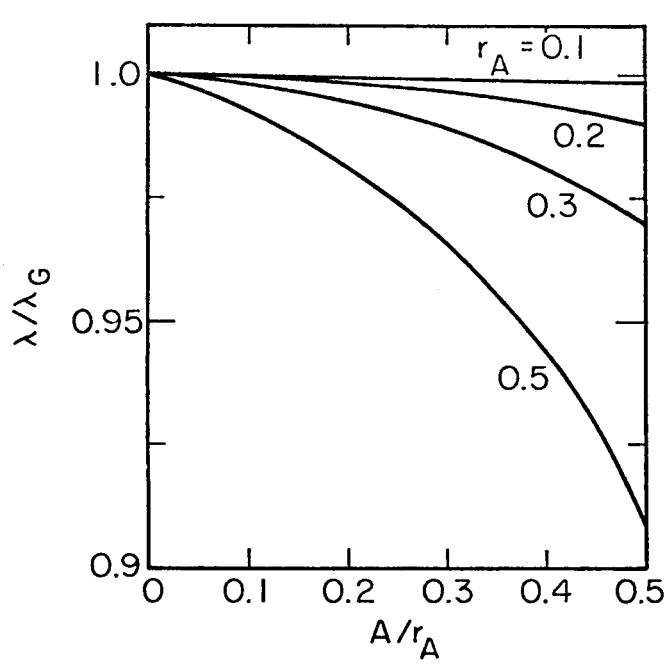

Fig. 10. Eigenvalues for the mass transfer problem in a sinusoidal PCT normalized with respect to the Graetz problem.

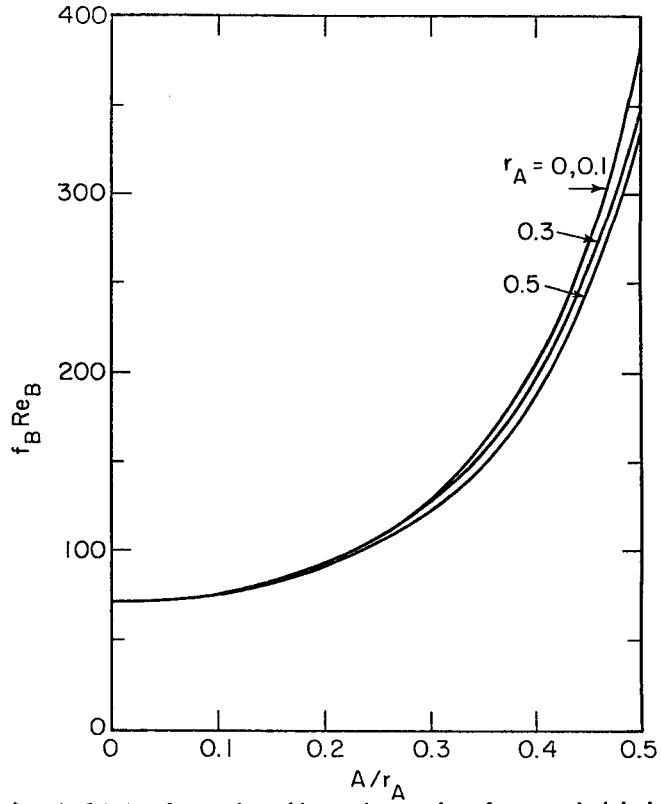

Fig. 9. Friction factor, Reynolds number product for a packed bed modeled as an array of sinusoidal PCT.

Sherwood number for any periodic tube. Only the stream function need be known. Calculated results are presented for the sinusoidal PCT of Figure 2 in creeping flow. The results are a function of the two dimensionless geometric parameters r_A and A/r_A.

Figure 10 presents the first eigenvalue of Equation (21) normalized with respect to the first eigenvalue of the straight tube Graetz problem ($\lambda_G = 0.91419$). This plot

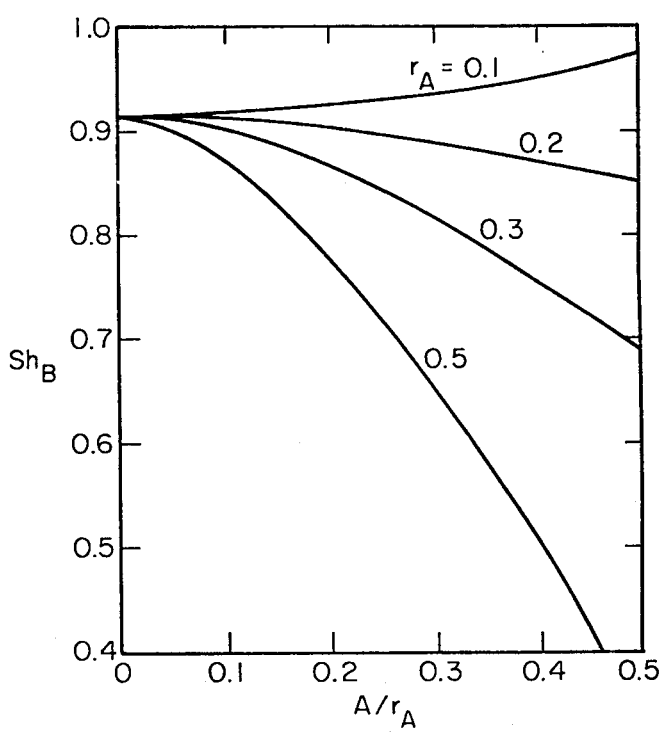

Fig. 11. Asymptotic Sherwood number for a packed bed modeled as an array of sinusoidal PCT.

can also be interpreted as the ratio of the asymptotic Sherwood number (*based on the average radius* r_{Ad}) of a sinusoidal PCT to that in a straight tube of radius r_{Ad}.

Figure 11 presents the Sherwood number for a packed bed modeled as an array of sinusoidal PCT. The concentration drop across the bed can be written as

$$\ln c_o/c_L = Sh_B \frac{aL_B}{\epsilon} Pe_B \tag{31}$$

Figure 10 shows a monotonic behavior of the eigenvalues with r_A and A/r_A. However, the bed-Sherwood number shows different trends for small and large r_A. For small r_A, Sh_B increases with A/r_A, whereas for larger r_A this trend reverses itself. This effect is caused by the geometrical term in Equation (26).

The quantity $2\epsilon/a$ in Equation (26) is the standard definition for the equivalent radius of the bed. This defines the bed in terms of a straight cylinder network of radius $r_{eq,d}$ having the same surface area to empty volume ratio. The quantity $r_{Ad}^2[1 + (1/2)(A/r_A)^2]$ in the denominator of Equation (26) defines another equivalent radius r_{Vd}^2. This is the volumetric average radius for a sinusoidal PCT. For long skinny PCT (small r_A), the ratio $(r_{eq}/r_v)^2$ is greater than 1 and increases with A/r_A. Thus, for a bed composed of these tubes, the Sherwood number increases as A/r_A is increased. However, as r_A becomes larger, the ratio $(r_{eq}/r_v)^2$ becomes less than 1, and Sh_B decreases with A/r_A.

For most beds, r_A will be bounded approximately by $0.3 < r_A < 0.5$, while the A/r_A ratio will be in the range $0.2 < A/r_A < 0.5$, perhaps close to 0.33. Payatakes et al. report these parameters for a randomly packed bed of glass spheres as $r_A = 0.3$, $A/r_A = 0.36$, and for a bed of sand as $r_A = 0.31$, $A/r_A = 0.41$.

Sørenson and Stewart (1974) have calculated the asymptotic value of the Sherwood number in a simple cubic packed bed of uniform sized spheres. Their results yield $Sh_B = 0.619$. This information can be used in conjunction with the friction factor, Reynolds number product calculated by these same authors. This suggests that the PCT parameters for a simple cubic packing of spheres are $r_A \approx 0.5$ and $A/r_A \approx 0.33$. We expect this r_A value to be an upper limit for uniform spheres, since the simple cubic packing has the highest porosity of all sphere packing configurations.

No experimental packed bed heat or mass transfer correlations are known to the authors which demonstrate a transfer rate independent of velocity. Three factors can mask this asymptote: at very low velocities, axial dispersion may become important; at high flow rates, turbulence becomes important; and at the intermediate flow rates, the entire bed may be in the entry region (small aL). However, the asymptotic Sherwood number gives a conservative estimate useful for design purposes.

ACKNOWLEDGMENT

This work was supported by the U.S. Energy Research and Development Administration.

This paper was originally presented at the 1976 Fall Meeting of the Electrochemical Society, Inc., in Las Vegas, Nevada, and is published with permission of The Electrochemical Society, Inc.

NOTATION

a = specific interfacial area of bed, cm^{-1}
A = dimensionless wall oscillation amplitude, A_d/l
$A_k(z)$ = interior collocation coefficient functions
c_o = concentration of limiting reactant entering bed, mole/cm^2
c_L = concentration of limiting reactant leaving bed, mole/cm^3
C = dimensionless reactant concentration $(C_d - C_w)/(C_b - C_w)$
D = diffusion coefficient of reactant, cm^2/s
f_B = bed friction factor defined by Equation (9)
G = function of ψ defined by Equation (22)
h_ψ, h_ξ, h_θ = dimensionless metric factors
k_m = effective mass transfer coefficient of a bed, cm/s
L_B = length of bed, cm
l = length of PCT period, cm
$\mathcal{P}_B$ = pressure in bed
Pe = reactant Péclet number in a PCT, $2r_{Ad}\langle v_{Ad}\rangle/D$
Pe_B = bed Péclet number, v_s/aD
r = dimensionless radial coordinate, r_d/l
r_A = dimensionless average PCT radius, r_{Ad}/l
$r_{eq,d}$ = equivalent radius, $2\epsilon/a$
r_{Vd} = volumetric equivalent radius, $r_{Ad}\sqrt{1 + (1/2)(A/r_A)^2}$
r_w = dimensionless wall radius, r_{wd}/l
Re_B = bed-Reynolds number, v_s/av
Sh_B = bed-Sherwood number, $\epsilon k_m/aD$
v_s = superficial approach velocity, cm/s
$\langle v_{Ad}\rangle$ = average velocity in a tube of constant radius r_{Ad}, cm/s
v_r = dimensionless radial velocity, $v_{rd}/\langle v_{Ad}\rangle$
v_z = dimensionless axial velocity, $v_{zd}/\langle v_{Ad}\rangle$
v_ξ = dimensionless streamwise velocity, $\sqrt{v_z^2 + v_r^2}$
z = dimensionless axial coordinate, z_d/l

Greek Letters

β = constant defined by Equation (10), cm^{-1}
ϵ = bed porosity
ν = kinematic viscosity, cm^2/s
ξ = streamwise coordinate
ρ = transformation coordinate of Equation (28)
η = $r/r_w(z)$
θ = polar coordinate
λ = eigenvalue of Equation (21)
ψ = dimensionless normalized stream function, $-2\psi_d/r_{Ad}^2\langle v_{Ad}\rangle$
$\{\phi_k\}$ = complete set of functions

Subscripts

d = dimensional quantity
b = bulk

APPENDIX A

E^4 operator in (η, z) coordinate system

$$E^4 = \frac{1}{r_w^4}[1 + \eta^2(r'_w)^2]^2 \frac{\partial^4}{\partial\eta^4} - \frac{4\eta}{r_w^3} r'_w[1 + \eta^2(r'_w)^2]$$

$$\frac{\partial^4}{\partial z\partial\eta^3} + \frac{1}{r_w^2}[2 + 6\eta^2(r'_w)^2] \frac{\partial^4}{\partial z^2\partial\eta^2} - \frac{4\eta}{r_w} r'_w \frac{\partial^4}{\partial z^3\partial\eta}$$

$$+ \frac{\partial^4}{\partial z^4} + \frac{1}{r_w^4}\left[-\frac{2}{\eta} + 10\eta(r'_w)^2 + 12\eta^3(r'_w)^4 - 2\eta r_w r''_w \right.$$

$$\left. - 6\eta^3 r_w(r'_w)^2 r''_w \right] \frac{\partial^3}{\partial\eta^3} + \frac{1}{r_w^3}[-4'_w - 24\eta^2(r'_w)^3$$

$$+ 12\eta^2 r_w r'_w r''_w] \frac{\partial^3}{\partial z\partial\eta^2} + \frac{1}{r_w^2}\left[12\eta(r'_w)^2 - 6\eta r_w r''_w - \frac{2}{\eta} \right]$$

$$\frac{\partial^3}{\partial z^2\partial\eta} + \frac{1}{r_w^4}\left[4(r'_w)^2 - 2r_w r''_w + \frac{3}{\eta^2} + 36\eta^2(r'_w)^4 \right.$$

$$+ 3\eta^2 r_w^2 (r''_w)^2 - 36\eta^2 r_w (r'_w)^2 r''_w + 4\eta^2 r_w^2 r'_w r'''_w \Big] \frac{\partial^2}{\partial \eta^2}$$

$$\frac{1}{r_w^2}\Big[24\eta r'_w r''_w - \frac{24\eta}{r_w}(r'_w)^3 + \frac{4}{\eta r_w} r'_w - 4\eta r_w r'''_w \Big]$$

$$\frac{\partial^2}{\partial z \partial \eta} + \frac{1}{r_w^4}\Big[-\frac{3}{\eta^3} - \frac{4}{\eta}(r'_w)^2 + 24\eta (r'_w)^4$$

$$- 36\eta r_w (r'_w)^2 r''_w + 8\eta r_w^2 r'_w r'''_w + 6\eta r_w^2 (r''_w)^2$$

$$+ \frac{2}{\eta} r_w r''_w - \eta r_w^3 r_w^{(iv)} \Big] \frac{\partial}{\partial \eta}$$

LITERATURE CITED

Batra, V. K., G. D. Fulford, and F. A. L. Dullien, "Laminar Flow through Periodically Convergent-Divergent Tubes and Channels," *Can. J. Chem. Eng.*, **48**, 622 (1970).

Bennion, D. N., and J. Newman, "Electrochemical removal of copper ions from very dilute solutions," *J. Appl. Electrochem.*, **2**, 113 (1972).

Bird, R. B., W. E. Stewart, and E. N. Lightfoot, *Transport Phenomena*, Wiley, New York (1960).

Dullien, F. L., "Single Phase Flow through Porous Media and Pore Structure," *Chem. Eng. J.*, **10**, 1 (1975).

———, and M. I. S. Azzam, "Flow Rate-Pressure Gradient Measurements in Periodically Non Uniform Capillary Tubes," *AIChE J.*, **19**, 222 (1973).

Fedkiw, P. S., Ph.D. thesis, in preparation.

Finlayson, B. A., *The Method of Weighted Residuals and Variational Principles*, Academic Press, New York (1972).

Houpeurt, A., "Sur l'Écoulement des Gaz dans les Milieux Poreux," *Rev. Inst. Fr. Petrole Ann. Combust. Liquides*, **14**, 1467 (1959).

Michaels, A. S., *AIChE J.*, **5**, 270 (1959).

Newman, J. S., *Electrochemical Systems*, Appendix C, Prentice-Hall, Englewood Cliffs, N.J. (1973*a*).

———, "The Fundamental Principles of Current Distribution and Mass Transport in Electrochemical Cells," in *Electroanalytical Chemistry*, Vol. 6, p. 187, Marcel Dekker, New York (1973*b*).

———, and W. Tiedemann, "Flow-Through Porous Electrodes," submitted to *Adv., Electrochem., and Electroeng.*, (1976).

Payatakes, A. C., C. Tien, and R. M. Turian, "A New Model for Granular Porous Media: Part 1. Model Formulation," *AIChE J.*, **19**, 58 (1973).

———, "Part 2. Numerical Solution of Steady State Incompressible Newtonian Flow Through Periodically Constricted Tubes," *ibid.*, 67 (1973).

Petersen, E. E., "Diffusion in a Pore of Varying Cross Section," *ibid.*, **4**, 343 (1958).

Sheffield, R. E., and A. B. Metzner, "Flow of Non Linear Fluids Through Porous Media," *ibid.*, **22**, 736 (1976).

Sheidegger, A. E., *The Physics of Flow Through Porous Media*, Macmillan, New York (1957).

Sørenson, J. P., and W. E. Stewart, "Computation of Forced Convection in Slow Flow through Ducts and Packed Beds—II Velocity Profile in a Simple Cubic Array of Spheres," *Chem. Eng. Sci.*, **29**, 819 (1974*a*).

———, "Computation of Slow Flow through Ducts and Packed Beds—III Heat and Mass Transfer in a Simple Cubic Array of Spheres," *ibid.*, 827 (1974*b*).

Villadsen, J. V., *Selected Approximation Methods for Chemical Engineering Problems*, Danmarke Tekniske Højskole, Copenhagen (1970).

———, and W. E. Stewart, "Solution of Boundary Value Problems by Orthogonal Collocation," *Chem. Eng. Sci.*, **22**, 1483 (1967).

Wilson, E. J., and C. J. Geankopolis, "Liquid Mass Transfer at Very Low Reynolds Numbers in Packed Beds," *Ind. Eng. Chem. Fundamentals*, **5**, 9 (1966).

Manuscript received December 21, 1976, and accepted January 11, 1977.

Multicomponent Liquid Phase Adsorption in Fixed Bed

J. S. C. HSIEH
RAFFI M. TURIAN
and
CHI TIEN

Department of Chemical Engineering and Materials Science
Syracuse University
Syracuse, New York 13210

Although multicomponent, liquid phase adsorption is often encountered in industrial application, most of the studies concerning fixed-bed sorption processes have been dealt primarily with systems containing one adsorbable species. The present work provides a numerical solution to the fixed-bed, multicomponent adsorption problem, taking into account both separately or in combination the effect of liquid and/or solid phase mass transfer resistance and of variation of the assumed governing adsorption isotherm. Numerical solutions of several example problems are presented and compared with results based on equilibrium theory and a simplified method developed by Cooney and co-workers previously (1972).

SCOPE

This work was undertaken in order to establish a rigorous general theoretical model pertaining to fixed-bed adsorption in multicomponent liquid systems. The non-equilibrium theory developed here is capable of accommodating, separately as well as in combination, the effects of liquid and/or solid mass transfer resistances and of variations in the form of the assumed governing adsorption isotherm, and it can therefore be used to estimate the interactive influences of these effects. Furthermore, the present theory can be used to assess the effectiveness of approximations based on the computationally convenient, though physically unrealistic, concepts of equilibrium or single solute lumping. The theory can be extended, in principle, to account for an increasing number of possible adsorbable species, and this makes it particularly apt for wastewater adsorption processes.

J. S. C. Hsieh is with the Scott Paper Company, Philadelphia, Pennsylvania. R. M. Turian is with the National Science Foundation on leave from Syracuse University.